Drug Design, Development and Therapy

Dovepress
open access to scientific and medical research

Open Access Full Text Article

ORIGINAL RESEARCH

Andrographolide Attenuates NLRP3 Inflammasome Activation and Airway Inflammation in Exacerbation of Chronic Obstructive Pulmonary Disease

Yan Yu[1,*], Ti-wei Miao[1,*], Wei Xiao[1], Bing Mao[1], Long-yi Du[1], Yan Wang[2], Juan-juan Fu[1]

[1]Division of Pulmonary Medicine, Department of Internal Medicine, Institute of Integrated Traditional Chinese and Western Medicine, West China Hospital, Sichuan University, Chengdu, Sichuan, 610041, People's Republic of China; [2]Research Core Facility, West China Hospital, Sichuan University, Chengdu, Sichuan, 610041, People's Republic of China

*These authors contributed equally to this work

Correspondence: Juan-juan Fu, Division of Pulmonary Medicine, Department of Internal Medicine, Institute of Integrated Traditional Chinese and Western Medicine, West China Hospital, Sichuan University, 37 Guoxue Street, Chengdu, Sichuan, 610041, People's Republic of China, Tel +86-18980606822, Email fu.juanjuan@scu.edu.cn

Purpose: The aim of this study is to uncover the anti-inflammatory propertity of andrographolide (AGP) in acute exacerbation of chronic obstructive pulmonary disease (AECOPD) and the underlying mechanisms related to the nucleotide-binding oligomerization domain-like receptor protein 3 (NLRP3) inflammasome pathway.

Methods: An in vivo experiment was conducted on murine model of AECOPD through endotracheal atomization of elastase and lipopolysaccharide (LPS). Intraperitoneal AGP was administered four times. NLRP3 inflammasome pathway molecules were examined using real-time quantitative polymerase chain reaction (RT-qPCR) and Western blot analysis. By using enzyme-linked immunosorbent assay (ELISA), we tested interleukin (IL)-1β levels in bronchoalveolar lavage fluid. An in vitro study was conducted to determine how AGP impacts the NLRP3 inflammasome in THP-1 derived macrophages. The levels of molecules involved in the pathway were measured. Furthermore, molecular docking analyses were carried out to investigate the interactions between AGP and pathway targets.

Results: In the in vivo study, NLRP3 inflammasome activation was observed in mice experiencing AECOPD. The administration of high-dose AGP demonstrated a mitigating effect on inflammatory cells infiltration in the lungs. Moreover, AGP administration effectively suppressed the expression of NLRP3, apoptosis associated speck-like protein that contains a CARD (PYCARD), cysteinyl aspartate-specific protease-1 (Caspase-1), IL-1β, and IL-18 at both the genetic and protein levels. In the in vitro experiment, IL-1β levels were significantly elevated in THP-1 derived macrophages with activated inflammasome compared to the control group. Furthermore, the downregulation of NLRP3, CASP1, and IL1B genes was observed upon the inhibition of NLRP3 expression through small interfering RNA (siRNA). AGP demonstrated inhibitory effects on the gene expression and protein levels of NLRP3, Caspase-1, and IL-1β. Additionally, molecular docking analysis confirmed that AGP exhibited a favorable binding affinity with all five targets of the pathway.

Conclusion: AGP effectively inhibited NLRP3 inflammasome activation and mitigated the inflammatory reaction of AECOPD both in animal models and in vitro experiments, highlighting the potential of AGP as a treatment for AECOPD with anti-inflammatory properties.

Keywords: andrographolide, NLRP3 inflammasome, IL-1β, chronic obstructive pulmonary disease

Introduction

Chronic obstructive pulmonary disease (COPD) is a global public health issue that is characterized by chronic respiratory symptoms (dyspnea, cough, and sputum production), persistent airway inflammation and airflow limitation.[1,2] According to findings from the China Pulmonary Health (CPH) study, individuals with spirometry-defined COPD in China are

Received: 19 January 2024
Accepted: 9 May 2024
Published: 24 May 2024

estimated to be 99.9 million, representing approximately 8.6% of the total population.[3] Moreover, according to the World Health Organization, COPD accounts for approximately 3 million deaths in 2019, making it the third most prevalent cause for death globally.[4] Patients with COPD occasionally experience sudden worsening in airway function and respiratory symptoms, known as acute exacerbation of COPD (AECOPD).[5] AECOPD has significant adverse consequences for patients, including poorer health status, expedited deterioration in lung capacity, faster disease progression, and increased mortality rates.[6–8] Aggravated airway and systemic inflammatory responses are hallmarks of AECOPD. Systemic corticosteroids are extensively utilized in the management of AECOPD due to their effectiveness in suppressing airway inflammation.[9] Nonetheless, the use of these medications is accompanied by various adverse effects, such as increased susceptibility to infections, hyperglycemia, and gastrointestinal bleeding, particularly with higher cumulative doses due to the recurrent nature of AECOPD.[10,11] Hence, the development of effective and targeted anti-inflammatory pharmacotherapy for AECOPD is urgently needed.

An inflammasome is a multiprotein complex located in the cytosol that activates potent inflammatory mediators. The NOD-like receptor family pyrin domain-containing 3 (NLRP3) inflammasome plays a crucial role in the innate immune system by providing the defense against invading pathogens and cellular damage. The structure comprises of three components: a leucine-rich repeat located at the end of the sequence, a central domain called NACHT with ATPase activity responsible for nucleotide-binding and oligomerization, and a pyrin domain (PYD) positioned at the beginning of the sequence.[12,13] When activated, NLRP3 attaches to the apoptosis associated speck-like protein that contains a CARD (PYCARD/ASC). Then, ASC engages with the cysteinyl aspartate-specific protease-1 (Caspase-1), leading to the NLRP3–ASC–pro-Caspase-1 complex, commonly referred to as the inflammasome.[14] As this complex facilitates pro-Caspase-1 cleavage to its active form, interleukin (IL)-1 and IL-18 are released more readily, which trigger an inflammatory response.[15–17]

It has been shown in recent studies that the NLRP3 inflammasome contributes to persistent inflammation in the airways and to the progression of COPD.[18–20] According to clinical studies, molecules related to the NLRP3 pathway, such as NLRP3, Caspase-1, ASC, IL-1β, and IL-18, were found to be upregulated in AECOPD patients. This upregulation was observed in bronchial tissues, bronchoalveolar lavage fluid (BALF), sputum, serum and peripheral blood mononuclear cells.[18,21] The use of MCC950, a substance that inhibits the NLRP3 inflammasome, or siNLRP3, effectively reduced NLRP3 inflammasome mRNA and protein levels, as well as airway inflammatory infiltration and lung damage in IAV-infected COPD rats, indicating the crucial role of NLPR3 inflammasome activation in AECOPD.[22] Consequently, targeting the NLRP3 inflammasome may represent a promising therapeutic approach for AECOPD.[23]

Recently, it has been demonstrated that a range of plants and their refined components possess anti-inflammatory characteristics. Among these plants, Andrographis paniculata (Burm.f.) Nees of Acanthaceae family, a plant cultivated throughout China, has been used for preventing and treating upper respiratory tract infection, pneumonia, and colitis due to its cleansing and detoxifying properties.[24] In Andrographis paniculata (Burm.f.) Nees, the major bioactive compound is andrographolide (AGP), a labdane diterpenoid with anti-inflammatory, antioxidative and antiviral properties.[25–27] It has been demonstrated that the underlying anti-inflammatory mechanisms of AGP may be linked to the NF-κB, P38-MAPK, PIK3/AKT, JAK/STAT pathways.[27–30] Importantly, AGP exerted its anti-inflammatory effects by impeding NLRP3 inflammasome activation.[31,32] Previous research has also indicated that AGP could suppress CSE-induced IL-1β production in RAW 264.7 cells, a murine macrophage cell line, thereby attenuating respiratory inflammation.[33] Additionally, AGP treatment has been found to significantly decrease IL-1β levels in BALF of mice exposed to cigarette smoke and atypical Haemophilus influenzae infection.[34] Considering the significant involvement of IL-1β in the airway inflammation of AECOPD which mainly produced by NLRP3 inflammasome activation, whether AGP could inhibit NLRP3 mediated IL-1β secretion in AECOPD and alleviate inflammatory response remains unclear. In this study, we hypothesized that AGP could suppress NLRP3 inflammasome activation to attenuate airway inflammation in AECOPD.

Materials and Methods

Reagents and Experimental Animals

AGP (>98% purity by HPLC) was acquired from Guidechem (#5508-58-7, Shanghai, China), and was dissolved in dimethyl sulfoxide (DMSO, #D8418, Sigma, USA) for experiment. The study adhered to the National Institute of Health

Guide for the Care and Use of Laboratory Animals and received approval from the Animal Ethics Committee of West China Hospital of Sichuan University (2018126A). The research involving animals was carried out following with the Animal Research: Reporting In Vivo Experiments Guidelines. A total of thirty-six male C57BL/6 mice (Jiangsu Jicuiyaokang Biotechnology Co., Ltd, China), aged 8–10 weeks and weighing 18–22g, were housed in the animal experiment center under a 12-hrs light/dark cycle, with 50% relative humidity and room temperature maintained at 21˚C ± 2˚C. There was always food and water available to them. Six mice were randomly assigned to each of the following groups: control group, COPD group, COPD+ lipopolysaccharide (LPS) (AECOPD group), COPD+LPS +DMSO (AECOPD-DMSO group), COPD+LPS+AGP of low dose (AECOPD-AGP 5mg/kg group), and COPD+LPS +AGP of high dose (AECOPD-AGP 10mg/kg group).

COPD Model Establishment and Treatment

To create the COPD model, porcine pancreas elastase (#E1250, Sigma, USA) and LPS (#L8274, Sigma, USA) were given via endotracheal atomization at a concentration of 0.02 U elastase and 1 μg LPS in 50 μL phosphate buffer saline (PBS), once every week for a total of 4 weeks. The control group, on the other hand, received treatment with 50 μL PBS. The lungs and BALF were collected from both the COPD and control groups, one week after the final LPS/elastase stimulation. In the fifth week, the AECOPD group was created by intratracheal stimulation with LPS (10 μg LPS in 50 μL PBS), building upon the COPD group. To ensure the safety of intraperitoneal injection in mice, a maximum concentration of 10 mg/kg of AGP was determined to be soluble in 200 μL PBS with 1% DMSO and 1% Tween. In order to investigate the dose effect of AGP, a low concentration of 5 mg/kg was chosen for our study. Mice in the AGP of low dose (5 mg/kg AGP dissolved in 200 μL PBS with 1% DMSO and 1% Tween) and high dose (10 mg/kg) groups received intraperitoneal injections of AGP 2 hrs prior to the final LPS stimulation in the fifth week. Following the initial AGP treatment, subsequent administrations were given every 12 hrs for a total of three times. Mice belonging to the DMSO group received an injection of 200 μL PBS containing 1% DMSO and 1% Tween. The mice were euthanized 48 hrs after the last LPS aerosol administration for analysis in the AECOPD, AECOPD-AGP, and DMSO groups.

Measurement of Lung Function

The mice were administered anesthesia using 2% sodium pentobarbital (80 mg/kg). Following anesthesia, the mice underwent tracheostomy and were positioned on a Buxco lung function test system (Saint Paul, USA). Various lung function parameters including forced expiratory volume at 100 ms (FEV_{100}), forced expiratory volume at 200 ms (FEV_{200}), forced vital capacity (FVC), functional residual capacity (FRC), total lung capacity (TLC), and chord compliance (Cchord) were measured and recorded.

Collection of BALF and Inflammatory Cell Counts

Sterile ice-cold PBS was used to lavage the right lung of a mouse three times. After centrifugation, BALF was separated and the liquid was promptly stored at −80°C for subsequent assays. After being treated with lysis solution, the cells collected from BALF were reconstituted in 500 μL PBS. The number of cells was measured using the Countstar FL automated fluorescent cell analyzer (ALTT, China). Cell smears stained with Wright's staining allowed for the identification of neutrophils, macrophages, and lymphocytes. A minimum of 200 cells from five randomly chosen perspectives in each section were meticulously examined and tallied by two proficient, impartial researchers who were unaware of the interventions.

Histopathological Assessment

Samples of lung tissue, preserved in a neutral 10% formalin solution, were subjected to paraffin embedding and slicing (5 μM), followed by staining with hematoxylin and eosin. Subsequently, the extent of lung inflammation lung inflammatory lesions was assessed by utilizing a numerical scale that included the alveolar septal infiltrate score, perivascular infiltrate score, and peribronchiolar infiltrate score.[35] A trained histologist, unaware of the experimental details, evaluated the histologic inflammation score.

THP-1 Monocytes Culture and Polarization into Macrophages

THP-1, a cell line derived from human monocytic leukemia, was acquired from the National Collection of Authenticated Cell Culture located in Shanghai, China. The cells were grown in RPMI 1640 medium (#11875093, Invitrogen, USA) with the addition of 10% fetal bovine serum (#10099-141, Gibco, USA) and 1% (v/v) penicillin/streptomycin (#1719675, Gibco, USA) and kept at 37°C, 5% CO2 in a humid incubator. To achieve the differentiation of THP-1 monocytes into macrophages, the subsequent procedures were employed. In short, THP-1 cells (5×10^5/well) were placed in 6-well plates and exposed to 100 ng/mL of phorbol 12-myristate 13-acetate (PMA, #P1585, Sigma, USA) for 24 hrs. Afterwards, the RPMI 1640 medium supplemented with LPS (100 ng/mL) was used to replace the culture medium, and the cells were incubated for 24 hrs.

Assessment of Cell Viability

Cell viability was assessed using the 3-(4,5-dimethylthiazol-2-yl)-2,5-diphenyltetrazolium bromide (MTT, #M5655, Sigma, USA) reduction assay. After treatment, the medium was removed and the cells were washed with cold PBS. The cells were then incubated with MTT (5 mg/mL) in dulbecco's modified eagle medium (DMEM) at 37°C for 4 hrs. The medium was subsequently eliminated, and 150 μL DMSO was added to dissolve the formazan. After centrifugation, the supernatant of each sample was transferred to 96-well plates and the absorbance was read at 490 nm. The absorbance in cultures treated with 0.1% DMSO was regarded as 100% cell viability.

Transfection

THP-1 cells were placed onto 6-well plates and differentiated into macrophage-like cells with PMA for 24–48 hrs. Subsequently, LPS (100ng/mL) was added for 24 hrs when the cell confluency reached 60–80%, followed by the addition of ATP (5mmol/L) for 1 hr. Next, macrophages were transfected with 50 nmol/L NLRP3 Small interfering RNA (siRNA) using the NanoFect & Attractene HiPerFect transfection reagent (QIAGEN, Germany). We utilized the following NLRP3 siRNA sequences: sense, 5′- GUGCGUUAGAAACACUUCATT-3′, and antisense, 5′-UGAAGUGUUUCUAACGCACTT-3′. After a stimulation period of 48 hrs, the transfection efficiency was assessed using a fluorescence microscope, and both cells and supernatants were collected for future analysis.

AGP Treatment of THP-1 Derived Macrophages

AGP was dissolved in DMSO (80 μmol/L) and diluted with RPMI for further use. The macrophages were incubated with AGP (10, 20, 40 μmol/L) for 1 hr, followed by stimulation with LPS (0.1 μg/mL) for 24 hrs. Subsequently, the cells were stimulated with ATP (5 mmol/L) for 1 hr. The remaining cells, after removal of cell-free supernatants through centrifugation, were utilized for real-time quantitative polymerase chain reaction (RT-qPCR) and Western blot analysis. Supernatants were collected and the enzyme-linked immunosorbent assay (ELISA) kit was used to determine the concentration of IL-1β.

RT-qPCR

The study detected targets of the NLRP3 signaling pathway, namely *NLRP3, PYCARD, CASP1, IL1B*, and *IL18* genes, in different groups. The omega E.Z.N.A.® HP Total RNA Kit (#R6812-02, omega, USA) was used to isolate total RNA from lung tissue and THP-1 derived macrophages. The manufacturer's instructions were followed to ensure RNase-free conditions during the isolation process. Following that, the entire RNA was converted into cDNA using the PrimeScriptTM RT reagent Kit with gDNA Eraser (#RR047A, TaKaRa, Japan) according to the instructions provided in the manual. The comparative cycle threshold (Ct) method was used to calculate the relative mRNA expression. The gene's relative expression levels were normalized using the *β-actin/GAPDH* Ct value as an endogenous reference, employing a $2^{-\Delta\Delta Ct}$ relative quantification method. Tsingke Biotech (Beijing, China) synthesized primers, and their sequences can be found in Table 1.

Table 1 Primer Sequences for RT-qPCR

Gene	Forward (5'-3')	Reverse (5'-3')
In vivo		
NLRP3	GACTGGCAAAAGGCTGTG	AGTTTCTCCAAGGCTACCG
PYCARD	GGGCCATTCTGTTTCTCTC	CGTTCACCCTGGTTTTGT
CASP1	GCTCTGCGGTGTAGAAAAG	ATAGGTCCCGTGCCTTG
IL1B	AGTTGACGGACCCCAAA	TCTTGTTGATGTGCTGCTG
IL18	TCTGTGGTTCCATGCTTTC	TTGAGGCGGCTTTCTTT
β-actin	CAGGTCATCACTATTGGCAAC	TCTTTACGGATGTCAACGTCA
In vitro		
NLRP3	GAGGAAAAGGAAGGCCGACA	CCCGGCAAAAACTGGAAGTG
PYCARD	TTGGACCTCACCGACAAGCT	CGGTGCTGGTCTATAAAGTGCAG
CASP1	ACAGGCATGACAATGCTGCT	GCTGTCAGAGGTCTTGTGCT
IL1B	CAGAAGTACCTGAGCTCGCC	AGATTCGTAGCTGGATGCCG
IL18	AGCCTAGAGGTATGGCTGTAAC	AAAGGTCTCTCTCTTTTTCACAAGC
GAPDH	GGAGCGAGATCCCTCCAAAAT	GGCTGTTGTCATACTTCTCATGG

Abbreviations: RT-qPCR, reverse transcription quantitative polymerase chain reaction; NLRP3, nucleotide-binding oligomerization domain-like receptor protein 3; PYCARD, apoptosis-associated speck-like containing a CARD; CASP1, cysteinyl aspartate-specific protease-1; IL, interleukin.

Western Blot

Western blot was used to measure the protein levels of NLRP3, ASC, and Caspase-1 in the lung tissue of mice and macrophages derived from THP-1 cells. The protein phosphatase inhibitor cocktail (#P1266-1, Applygen Technologies, China), phenylmethylsulfonyl fluoride (PMSF) (#ST505, Beyotime Biotechnology, China), and radioimmunoprecipitation assay (RIPA) buffer (#P0013B, Beyotime Biotechnology, China) were used for total protein extraction. The concentration of the sample was determined using the BCA Protein Assay Kit (#23227, Thermo, USA). Proteins of the same quantities were subjected to electrophoresis using a 10% SDS-polyacrylamide gel (#PG112, Epizyme, China) and subsequently transferred onto polyvinylidene difluoride membranes (PVDF, Millipore, USA). PVDF filters were obstructed in 5% skimmed milk (Yili, China) for 1 hr at room temperature. After that, they were incubated with primary antibodies, which included rabbit anti-NLRP3 (#15101S, 1:500, Cell Signaling Technology, USA), rabbit anti-ASC (#67824S, 1:1000, Cell Signaling Technology, USA), and rabbit anti-Caspase-1 (#24232S, 1:1000, Cell Signaling Technology, USA) overnight at 4°C. After three washes with Tris-buffered saline (TBS-T) for five minutes each, the membranes were incubated at room temperature for 2 hrs with fluorescent-based secondary antibodies against rabbit IgG (#ZB-2301, 1:10000, ZSGB-BIO, China). Afterwards, an enhanced chemiluminescence technique (#1705060, Bio-rad, USA) was employed to observe protein expression, and the intensities of the bands were analyzed using ImageJ software (NIH, USA).

ELISA Analysis

After centrifugation, the collected supernatants from the BALF of mice and macrophages derived from THP-1 were obtained. IL-1β levels were measured with the ELISA kit (#MLB00C and #DLB50, R&D systems, USA), following the guidelines provided by the manufacturer.

Molecular Docking

To validate the binding affinity and interactions between AGP and targets (NLRP3, ASC, Caspase-1, IL-1β, and IL-18), molecular docking analysis was utilized. The 2D structures of AGP were retrieved from the PubChem database (https://pubchem.ncbi.nlm.nih.gov/), and while 3D structures of NLRP3, ASC, Caspase-1, IL-1β, and IL-18 were searched from the RCSB Protein Data Bank (PDB) (https://www.rcsb.org/). The PDBQT files were acquired through a series of steps including the elimination of water molecules, separation of proteins, addition of nonpolar hydrogens, and calculation of Gasteiger charges. AutoDock Tools and AutoDock Vina (version 1.1.2) were utilized to perform the docking procedure

of AGP with the targets and calculate the respective free binding energies. It is widely acknowledged that a lower binding energy between the ligand and receptor indicates a higher likelihood of interaction. Following the docking procedure, PyMOL (version 2.5.4) was employed to visualize the interaction and binding patterns between the most strongly bound group of molecules and the targets.

Statistical Analyses

Data analysis was performed using SPSS 23.0 software (SPSS Inc., USA) for statistical analyses, while figures were generated using GraphPad Prism 9 software (GraphPad 9.5.0). We evaluated the regularity of the data by conducting the Shapiro–Wilks test. The data were reported as means ± SEM or as the median (interquartile range) depending on the distribution types. To compare the two groups, either Student's *t*-test or Mann–Whitney *U*-test was utilized, whereas for equal variances involving multiple groups, ANOVA or Tukey's multiple-comparison test was employed. $P < 0.05$ was statistically significant.

Results

Effect of AGP Treatment on AECOPD Mice Model

COPD Mice Model

In comparison to the control group, the COPD group exhibited significant reductions in lung function indicators, specifically FEV_{100}/FVC and FEV_{200}/FVC, while FRC demonstrated a significant increase (Figure 1A). Additionally, the COPD group displayed significant increases in total inflammatory cell counts, neutrophil counts, macrophage counts, and lymphocyte counts, as depicted in Figure 1C, when compared to the control group. Furthermore, the mean linear intercept (MLI) in the COPD group was notably higher than that observed in the control group (Figure 1B).

AGP Relieved Inflammatory Cell Infiltration in AECOPD Mice

For in vivo study, the AECOPD group exhibited a significant increase in total inflammatory cell, neutrophil, macrophage, and lymphocyte counts in BALF compared to the COPD group. Following AGP treatment, there was a notable reduction in inflammatory cell counts and neutrophils in BALF compared to the AECOPD-DMSO group. This observation was consistent with H&E staining results of the AECOPD group, which revealed elevated neutrophil cell infiltration, hyperemia, edema, and thickened bronchial, presenting typical pathological changes associated with AECOPD (Figure 1C). Notably, the administration of a high dose of AGP treatment significantly mitigated inflammation infiltration, hyperemia, and bronchial thickening, indicating AGP relieved the lung pathological injury in AECOPD (Figure 1D and E).

AGP Inhibited NLRP3 Inflammasome Activation in AECOPD Mice

NLRP3, PYCARD, CASP1, IL1B, IL18 mRNA Expression

The results depicted in Figure 2A–E demonstrate a notable augmentation in the expression of *CASP1* and *IL18* mRNA in the COPD group when compared to the control group. Furthermore, the AECOPD group exhibited a significant upregulation in the levels of *NLRP3, PYCARD, CASP1, IL1B*, and *IL18* mRNA expression in comparison to the control group. High dose of AGP treatment (10mg/kg) significantly reduced *NLRP3, PYCARD, CASP1, IL1B*, and *IL18* mRNA expression compared to AECOPD-DMSO group.

NLRP3, ASC, Caspase-1 and IL-1β Protein Levels

As depicted in Figure 2F, increased protein levels of IL-1β in BALF were shown in AECOPD group compared to the control group. The administration of AGP (high dose) significantly reduced IL-1β protein levels compared to AECOPD-DMSO group.

As showed in Figure 3, the AECOPD group exhibited elevated protein levels of NLRP3, ASC, and Caspase-1 in comparison to the control group. NLRP3, ASC, and Caspase-1 protein expression levels were slightly decreased with a low dosage of AGP treatment, while a high dosage of AGP treatment significantly reduced these protein expression levels.

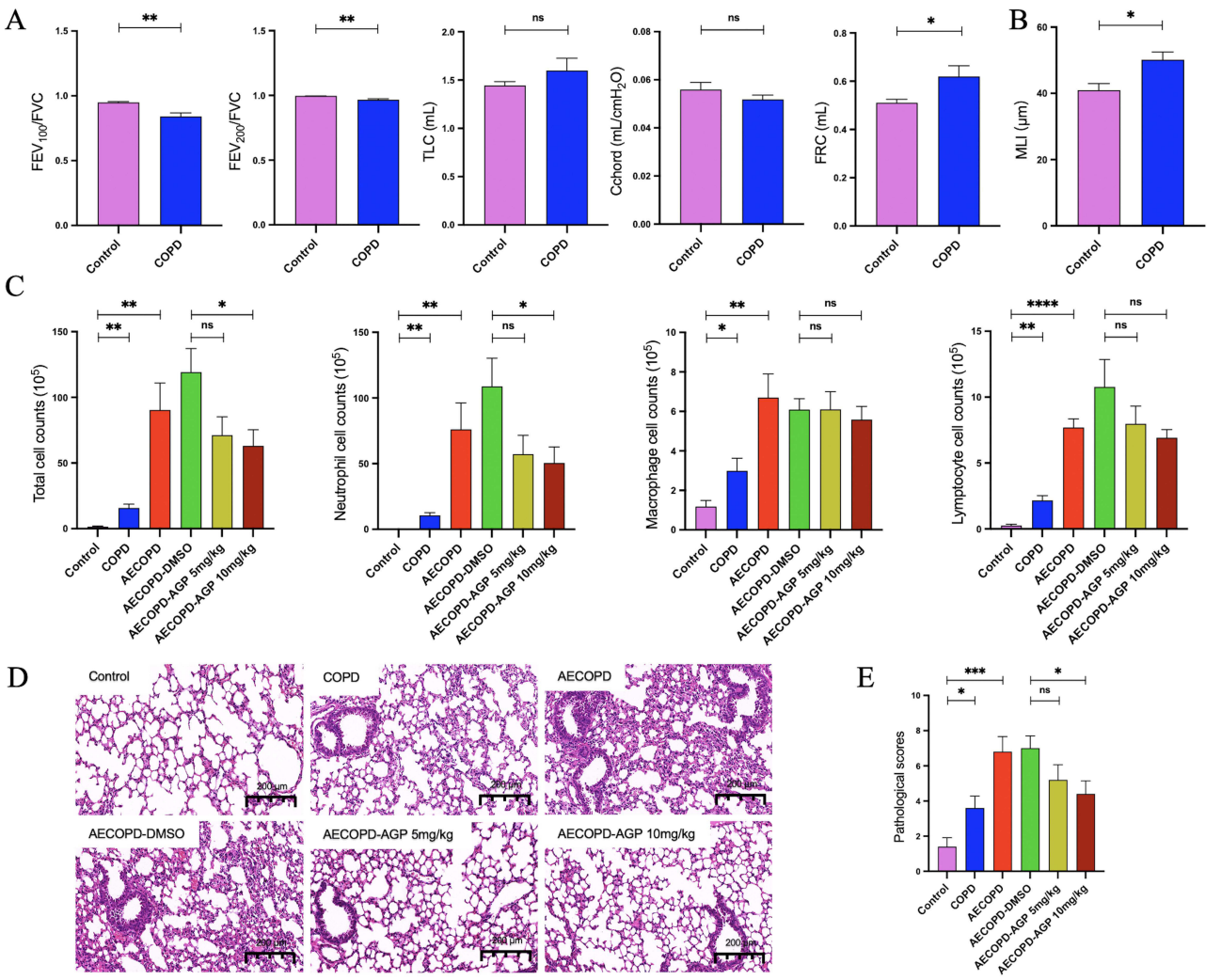

Figure 1 AGP inhibited inflammatory cell infiltration of the lungs in AECOPD mice. (**A**) Lung function indicators between control and COPD groups. (**B**) MLI between control and COPD groups. (**C**) Inflammatory cell counts in BALF for each group. (**D**) Representative pathological images of H&E staining on lung tissues. (**E**) Total pathological scores of lung tissues of each group. The results were presented as the mean ± SEM, n = 6, *P < 0.05; **P < 0.01; ***P < 0.001; ****P < 0.0001; ns, *P* > 0.05. **Abbreviations**: FEV_{100}, forced expiratory volume at 100 ms; FEV_{200}, forced expiratory volume at 200 ms; FRC, functional residual capacity; MLI, mean linear intercept; TLC, total lung capacity; Cchord, chord compliance; COPD, chronic obstructive pulmonary disease group; AECOPD, acute exacerbation of chronic obstructive pulmonary disease group; DMSO, dimethyl sulfoxide; AGP, andrographolide treatment group.

AGP Treatment Suppressed NLRP3 Inflammasome Activation on THP-1 Derived Macrophages

THP-1 Derived Macrophages

THP-1 cells were differentiated to macrophages by treatment with 100ng/mL PMA for 24–48 hrs and 100ng/mL LPS for 24 hrs, featured by larger cell size, irregular morphology, pseudopodia formation, and adherent growth (Figure 4A).

Small Interfering RNA (siRNA)

As shown in Figure 4B, the transfection efficiency was observed to be approximately 44–53% under a fluorescence microscope after transfection of 50 nmol/L NLRP3 siRNA into THP-1-derived macrophages for 48 hrs.

The concentration of IL-1β in the culture supernatant was measured using ELISA. The blank group had significantly lower IL-1β levels compared to the LPS+ATP group (Figure 5F). The IL-1β concentration in the supernatant of the NLRP3 siRNA group exhibited a decrease compared to that in the LPS+ATP group (Figure 5F), suggesting that inhibiting NLRP3 expression resulted in a downregulation of IL-1β secretion. Furthermore, the *NLRP3, CASP1*, and *IL1B* gene expression levels of the NLRP3 siRNA group were significantly decreased (Figure 5A, C and D), and NLRP3

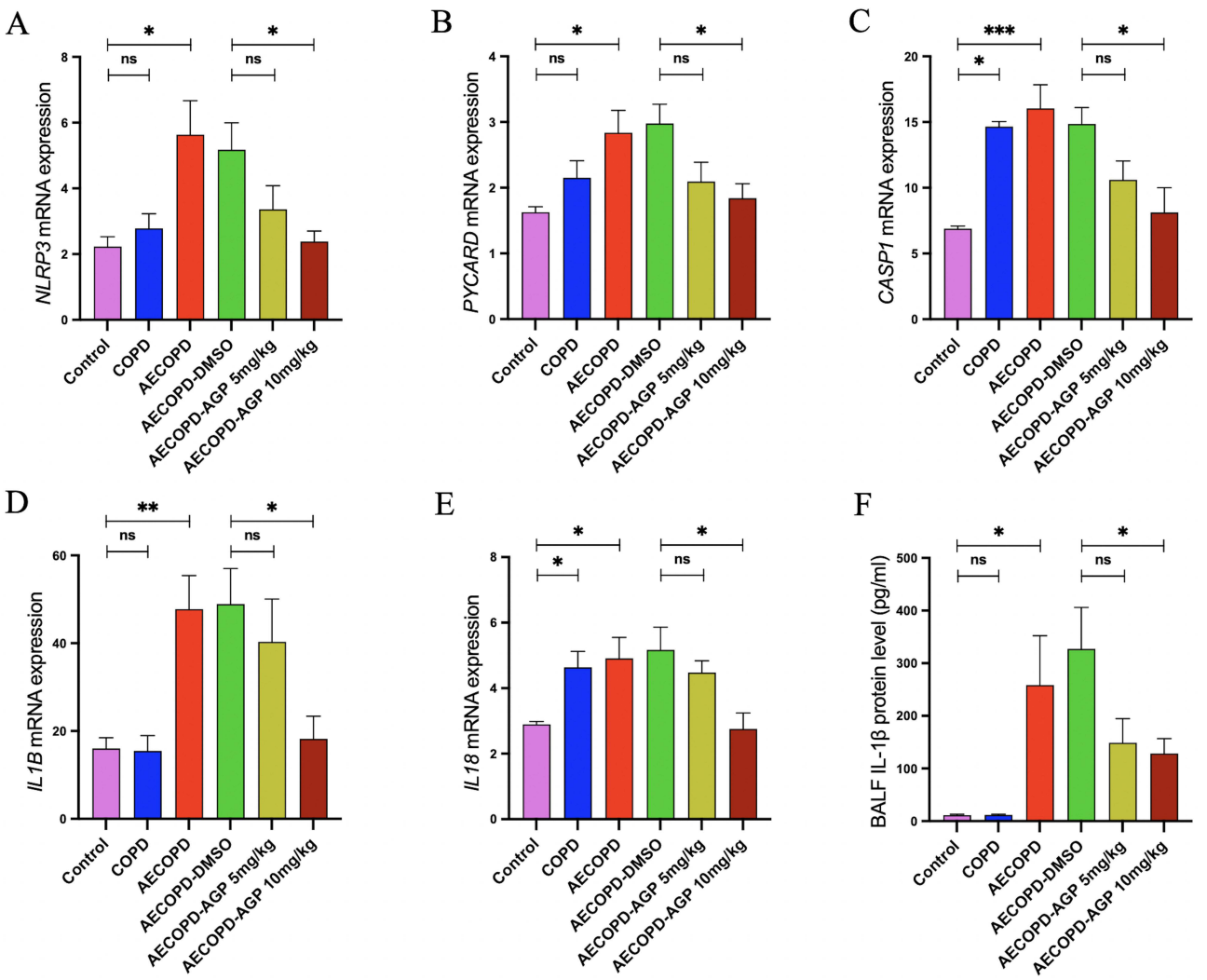

Figure 2 AGP downregulated the gene expression of NLRP3 signaling pathway in lung tissue and IL-1β protein levels in BALF of the AECOPD mice. (**A**–**E**) The mRNA expression of *NLRP3, PYCARD, CASP1, IL1B* and *IL18*, respectively. (**F**) The protein levels of IL-1β in BALF for each group. The results were presented as the mean ± SEM, n = 6, **P* <0.05; ***P* <0.01; ****P* <0.001; ns, *P* >0.05.

Abbreviations: COPD, chronic obstructive pulmonary disease group; AECOPD, acute exacerbation of chronic obstructive pulmonary disease group; DMSO, dimethyl sulfoxide; AGP, andrographolide treatment group; BALF, bronchoalveolar lavage fluid; NLRP3, nucleotide-binding oligomerization domain-like receptor protein 3; PYCARD, apoptosis associated speck-like protein that contains a CARD; CASP1, cysteinyl aspartate-specific protease-1; IL, interleukin.

and Caspase-1 protein expression were also downregulated (Figure 5F), which further confirmed that interfering NLRP3 gene expression can downregulate downstream gene and protein expression levels.

Cytotoxicity of AGP on THP-1 Derived Macrophages

Cell viability were not significantly impacted by intervention of AGP with concentration of 10, 20, and 40 μmol/L (Figure 4C) by MTT experiments, indicating the non-toxic effect of AGP on cells. The above concentrations were selected as the intervention concentration for in vitro study.

AGP Inhibited NLRP3-Mediated IL-1β Pathway Activation in THP-1 Derived Macrophages

Gene Expression Levels of NLRP3-Mediated IL-1β Pathway

The levels of *NLRP3* and *CASP1* expression were notably reduced by AGP treatment at concentrations of 10, 20, and 40 μmol/L, as depicted in Figure 5A–D. Furthermore, the groups that received 10 μmol/L and 20 μmol/L of AGP exhibited significantly reduced *IL1B* expression levels in comparison to the DMSO group. The gene expression of *PYCARD* in the AGP treatment group and NLRP3 group showed no notable changes in comparison to the LPS+ATP group.

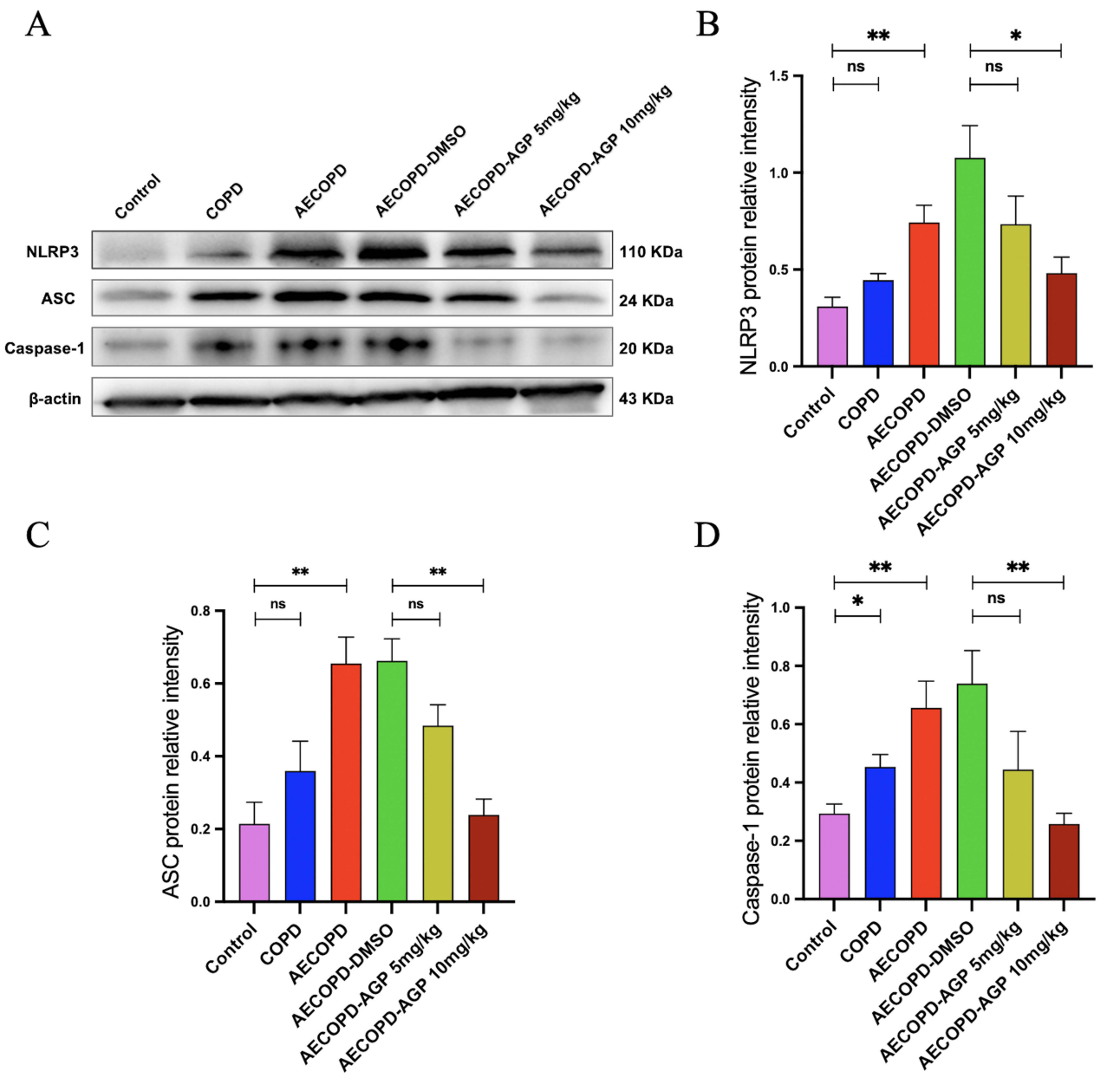

Figure 3 AGP inhibited protein levels of NLRP3 inflammasome pathway in lung tissue of AECOPD mice. (**A**) Western blot analysis of NLRP3, ASC, and Caspase-1 protein levels in the lung. (**B**–**D**) Corresponding grayscale statistics. The results were presented as the mean ± SEM, n = 4, $^{*}P < 0.05$; $^{**}P < 0.01$; ns, $P > 0.05$.
Abbreviations: COPD, chronic obstructive pulmonary disease group; AECOPD, acute exacerbation of chronic obstructive pulmonary disease group; DMSO, dimethyl sulfoxide; AGP, andrographolide treatment group; NLRP3, nucleotide-binding oligomerization domain-like receptor protein 3; ASC, apoptosis associated speck-like protein that contains a CARD; Caspase-1, cysteinyl aspartate-specific protease-1.

Protein Expression Levels of NLRP3-Mediated IL-1β Pathway

The protein expression levels of molecules associated with the NLRP3-mediated IL-1β pathway (NLRP3, ASC, Caspase-1) via Western blot in each experimental group. The findings indicated that NLRP3 and Caspase-1 protein levels were downregulated following treatment with varying concentrations of AGP (Figure 5E).

IL-1β levels in supernatants were detected using ELISA. Notably, treatment with 40 μmol/L of AGP significantly reduced the IL-1β levels, whereas no significant variances were detected in the groups treated with 10 and 20 μmol/L of AGP (Figure 5F).

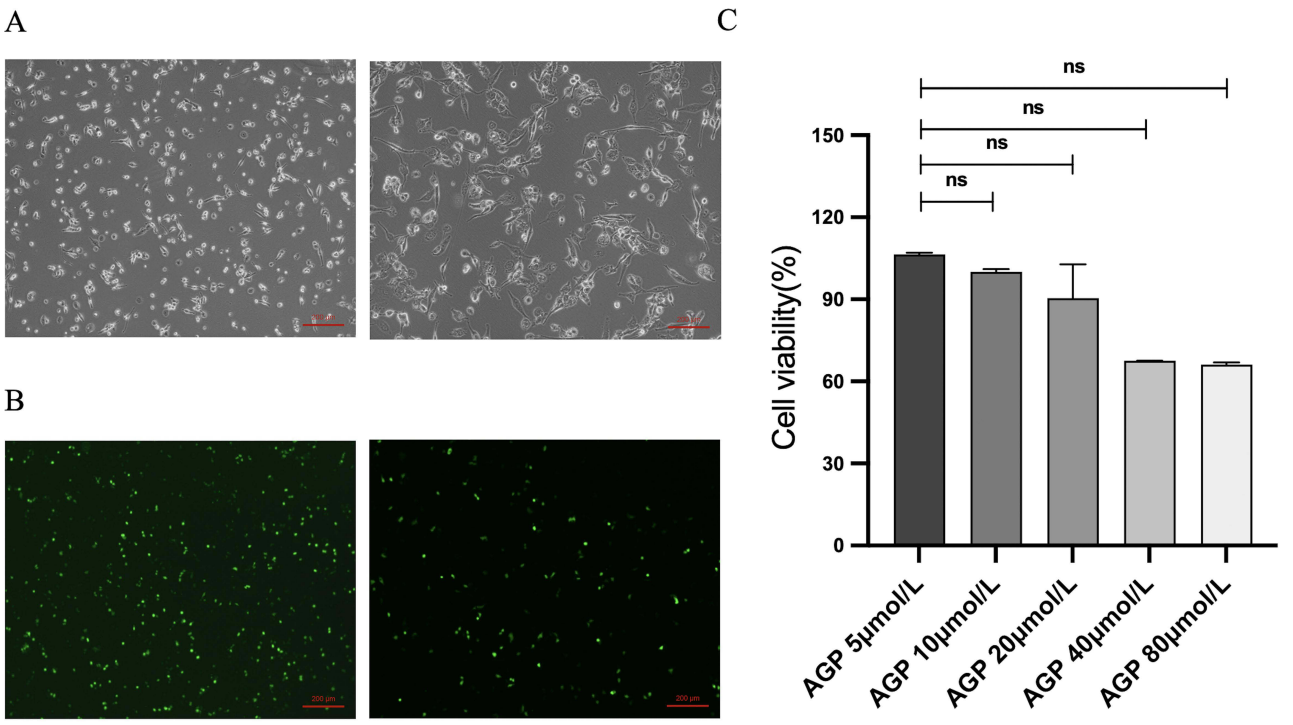

Figure 4 THP-1 induced macrophages and NLRP3 siRNA transfection. (**A**) THP-1 induced macrophages (left monocytes, right macrophages). (**B**) NLRP3 siRNA transfection of THP-1 derived macrophage (left before NLRP3 siRNA transfection, right after NLRP3 siRNA transfection). (**C**) Cell viability of THP-1 derived macrophages after the andrographolide treatment. Results were presented as median (interquartile range), n = 3, ns, $P > 0.05$.
Abbreviation: AGP, andrographolide treatment.

Exploring the Interactions and Possible Modes of Binding Between AGP and the NLRP3 Inflammasome Pathway

A molecular docking analysis was conducted to investigate and confirm the potential interactions and binding modes between AGP and the proteins associated with the NLRP3 inflammasome pathway. Figures 6A and S1–S4 (see Supplementary File) displayed the docking energies, indicating that AGP exhibited strong binding affinity with NLRP3, ASC, Caspase-1, IL-1β, and IL-18, as all the binding energies were below −5 kcal/mol. The stability of the binding conformation increased as the free binding energy decreased, and NLRP3 exhibited the strongest affinity for AGP. There were two pairs of hydrogen bonds, six pairs of hydrophobic interactions hydrogen bonds and one pair of salt bridge between AGP and NLRP3. Figure 6B and C displayed the depicted molecular binding models of NLRP3. In the complex AGP-NLRP3, AGP bound to a pocket on NLRP3 protein surrounded by amino acids LEU164, ARG167, ILE234, TYR381, PRO412, TRP416, SER161, SER163, and HIS522. There were hydrogen bonds with SER161 and SER163, salt bridges with HIS522 and hydrophobic interactions with LEU164, ARG167, ILE234, TYR381, PRO412 and TRP416. In summary, the main interaction between NLRP3 and AGP is salt bridge, hydrogen bond and hydrophobic action.

Discussion

Growing evidence has showed the involvement of NLRP3 inflammasome in the aggravation of inflammatory response during exacerbation of COPD.[36–38] In this study, we observed that treatment with AGP inhibited the activation of NLRP3 inflammasome and mitigated pulmonary inflammation in a mouse model of AECOPD. Additionally, we confirmed the inhibition of the NLRP3 inflammasome pathway by AGP in THP-1 derived macrophages. Furthermore, we identified the binding modes between AGP and potential targets of the NLRP3 signaling pathway, providing further evidence of AGP's interaction with NLRP3, particularly at the molecular level.

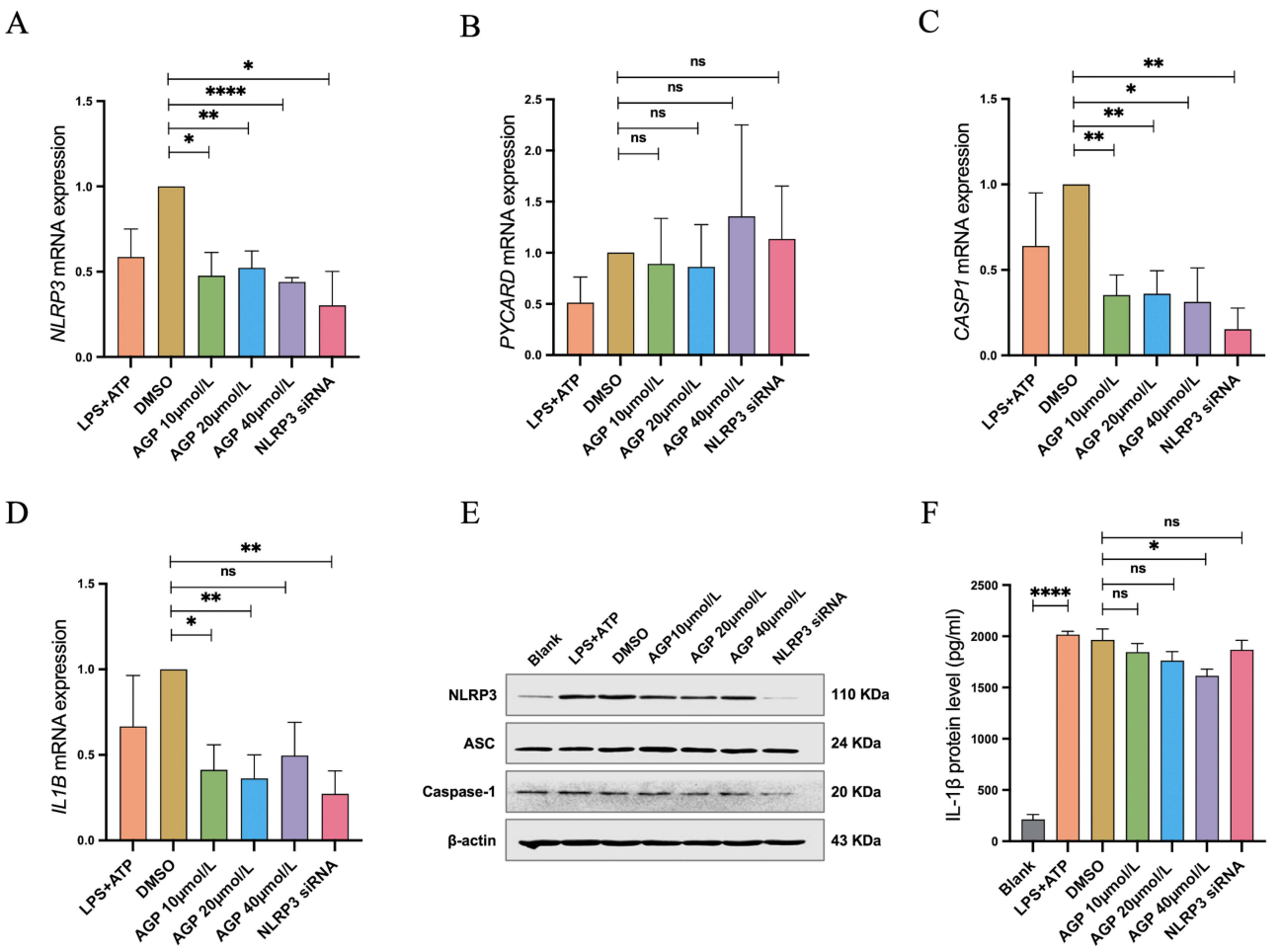

Figure 5 siRNA interference and AGP treatment inhibited the gene and protein expression levels of NLRP3 pathway in THP-1 derived macrophages. (**A**–**D**) The mRNA expression of *NLRP3, PYCARD, CASP1* and *IL1B*. (**E**) Western blot analysis of NLRP3, ASC, and Caspase-1 protein levels. (**F**) IL-1β concentration in the culture supernatant for each group. The results were presented as the mean ± SEM, n = 3, **P* < 0.05; ***P* < 0.01; *****P* < 0.0001; ns, *P* > 0.05.

Abbreviations: LPS, lipopolysaccharide; DMSO, dimethyl sulfoxide; AGP, andrographolide treatment. NLRP3, nucleotide-binding oligomerization domain-like receptor protein 3; PYCARD, apoptosis associated speck-like protein that contains a CARD; CASP1, cysteinyl aspartate-specific protease-1; IL, interleukin; siRNA, small interfering RNA.

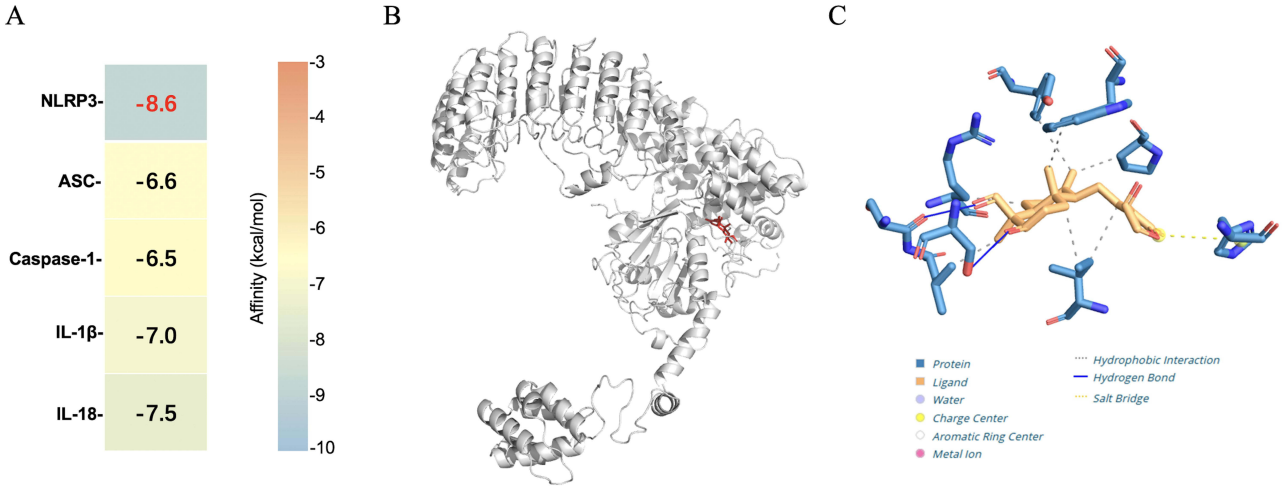

Figure 6 Interactions and potential binding modes between AGP and molecules related to NLRP3 inflammasome pathway. (**A**) The docking score of AGP with the targets of NLRP3, ASC, Caspase-1, IL-1β and IL-18. (**B**) Representative 3D binding model of AGP to NLRP3. (**C**) representative 2D model of the binding of AGP to NLRP3.

Abbreviations: NLRP3, nucleotide-binding oligomerization domain-like receptor protein 3; ASC, apoptosis associated speck-like protein that contains a CARD; Caspase-1, cysteinyl aspartate-specific protease-1; IL, interleukin.

Prior clinical investigations have presented proof of the substantial participation of NLRP3 inflammasome in the pathogenesis and worsening of COPD. Faner et al discovered that COPD patients exhibited elevated levels of NLRP3 mRNA expression in their lung tissue in comparison to healthy individuals.[21] Furthermore, in AECOPD patients, the expression of *NLRP3, PYCARD, CASP1, IL1B*, and *IL18* were found to be upregulated in both bronchial tissues and peripheral blood mononuclear macrophages, compared to stable COPD patients and healthy smokers.[18] Moreover, patients with AECOPD exhibited notably higher levels of IL-1β and IL-18 in spontaneous sputum, serum, and BALF supernatants, as evidenced by previous studies.[18,21] Similarly, significantly increased IL-1β levels were also observed in a rat model induced by influenza A virus.[39,40] IL-1β has been inked to with frequent exacerbations, prolonged smoking duration, elevated neutrophil counts, and increased C-reactive protein levels in patients with COPD.[40–42] Further, IL-1R deficient mice had significantly less airway neutrophils following exposure to cigarette smoke, indicating the crucial involvement of IL-1β in the acute exacerbations in COPD.[43,44] The present study has corroborated these findings by demonstrating the clear activation of NLRP3 inflammasome in the AECOPD mouse, and has further identified AGP as an effective inhibitor of its activation.

Within the lung, monocytes and macrophages serve as the primary effector cells of NLRP3.[45] Alveolar macrophages, in particular, play a key role in the inflammation and progression of COPD.[46] In response to bacterial, viral, and external stimuli, macrophages have been observed to generate IL-1β, which subsequently influences the influx of neutrophils and recruitment of monocytes, thereby worsening the inflammatory response in exacerbation of COPD.[47–49] Given the restricted availability of macrophages that can be obtained from BALF samples in mice, our study used THP-1 monocyte-derived macrophage, a commonly used model for investigating macrophages, particularly in COPD.[50–52] In this study, the NLRP3 inflammasome was activated through stimulation with LPS+ATP, leading to notable elevations in IL-1β levels in THP-1-derived macrophages. Furthermore, administration of AGP resulted in the suppression of the NLRP3 signaling pathway and a reduction in IL-1β secretion. These findings provided additional evidence that AGP has the ability to inhibit the NLRP3 inflammasome pathway in AECOPD.

Various exogenous activators, including cigarettes smoke, air pollution particles, silica crystals, and asbestos fibers, as well as endogenous molecules like LPS, pathogen-associated molecular pattern, tumour necrosis factor α, or IL-1β, can trigger the activation of the NLRP3 inflammasome. Additionally, NLRP3 inflammasome can be activated by viral, bacterial, or fungal infections, which have been identified as crucial factors contributing to exacerbations in patients with COPD.[53–56] For example, pneumolysin, which is a crucial factor for the virulence of Streptococcus pneumoniae, was discovered to be a strong NLRP3 inflammasome activator.[54] Furthermore, the stimulation of murine macrophages with Nontypeable Haemophilus influenzae has been observed to result in the activated NLRP3 inflammasome and the subsequent release of IL-1β through Caspase-1-dependent mechanisms.[55] Blocking NLRP3 activation decreased the levels of IL-1β and IL-18 in mice infected with influenza A virus and improved their survival.[56] Gram-negative bacteria produce LPS as a major microbial mediator, while Toll-like receptors (TLRs) serve as the transmembrane transduction receptors that initiate extracellular-to-intracellular communication.[57] Through its direct engagement with TLR4, LPS activates the NF-κB ligands for TLRs or cytokine receptors, activating the transcription factor NF-κB, which then activates NLRP3 and upregulates pro-IL-1β.[58] These findings elucidated a significant respiratory infection mechanism by which the main triggers for exacerbation of COPD aggravated lung inflammation during AECOPD by the activation of NLRP3 inflammasome.

The involvement of NLPR3 inflammasome in the observed inflammatory response has prompted extensive research on the targeting of pathway antagonists, which showed the amelioration of inflammatory cell infiltration and inflammatory molecules in COPD associated with NLRP3 inhibition, both in vivo and in vitro.[59–69] Studies focusing on therapeutic agents that directly target the NLRP3 inflammasome pathway have shown their effectiveness in COPD. For example, MCC950, a specific NLRP3 inhibitor, has demonstrated its ability to inhibit the activation of NLRP3 inflammasome, suppressed the IL-1β release and NLRP3-induced ASC oligomerization that alleviate inflammation of lung tissues in LPS-induced COPD mice models.[65,70] Recently, Zhang et al showed that VX-765, a specific Caspase-1 inhibitor, decreased levels of Caspase-1, IL-1β, IL-18, and lactate dehydrogenase in human bronchial epithelial cells following exposure to cigarette smoke extract.[66] On the other hand, there were also many other indirect NLPR3 inflammasome antagonists, including LP17 (a specific inhibitor of TREM-1),[64] melatonin,[60,61] histidine,[62] BML-111

(an agonist of lipoxin receptor),[59] (–)-Epicatechin (a type of flavonoid).[63] For example, histidine inhibited the NLRP3 inflammasome activation via the SIRT1-dependent pathway.[62] Despite the potential effects demonstrated by these therapeutic agents in COPD disease models, there remained a lack of specific mechanistic understanding and clinical application of these substances. Furthermore, trials have been carried out to evaluate the effectiveness of inhibitors targeting the NLRP3 pathway, including Canakinumab (an anti-human IL-1β monoclonal antibody),[69] MEDI2338 (an anti-human IL-18 monoclonal antibody)[68] or MEDI8968 (an anti-human IL-1R1).[67] Regrettably, these experiments did not reveal identify clinical improvements in COPD patients, compared with placebo. A recent study assessing the efficacy of DFV890, a novel NLRP3 inhibitor, in the treatment of coronavirus-associated acute respiratory distress syndrome demonstrated that early clearance of SARS-CoV-2, improved clinical outcomes, reduced fatal events, and enhanced in-hospital outcomes were observed with the use of DFV890.[71] However, it is crucial to acknowledge that currently there are no drugs of antagonists for NLRP3 pathway that are available on the market.

AGP, a naturally occurring labdane diterpenoid, has demonstrated protective effects by acting as an anti-inflammatory and immunomodulatory agent. It has also been proven to have therapeutic benefits for conditions such as intestinal inflammation, colitis, acute lung injuries, and respiratory infections.[72] Previous studies showed that AGP inhibited CSE-stimulated IL-1β production in vitro[33] and reduced IL-1β levels in BALF in Haemophilus influenzae infected COPD model mice.[34] In line with these discoveries, our study revealed that AGP intervention significantly downregulates IL-1β gene and protein expression in LPS/elastase induced AECOPD mice model and THP-1 derived macrophages. Importantly, the present study demonstrated that AGP inhibited NLRP3 inflammasome activation, which serves as the upstream pathway for IL-1β production. Besides, traditional Chinese medicine (TCM) has gained growing attention as a potential treatment for COPD, owing to its multi-target and multi-pathway action mechanisms, which distinguish it from Western medicines.[73,74] Notably, monomer compounds derived from TCM hold significant potential as valuable assets for the discovery of innovative reagents, given their exceptional biological activity and greater structural diversity in comparison to synthetic compounds.[75] In addition to the general advantages of monomers, AGP possessed the advantageous characteristics of low toxicity, ease of acquisition, and cost-effectiveness, rendering it extensively utilized in the treatment of diverse inflammatory conditions. Therefore, AGP could be a natural compound as regulators of NLRP3 Inflammasome-mediated pathway for anti-inflammatory therapy in AECOPD.

Molecular docking, a crucial technique for predicting molecular interactions between ligands and targets, is widely employed to investigate the mechanisms underlying such interactions.[76] In order to conduct a more comprehensive investigation into the molecular-level ligand–target interactions between AGP and NLRP3 inflammasome, we also further found that AGP exhibited a favorable binding affinity towards five targets associated with the NLRP3 inflammatory pathway, as determined through molecular docking analysis. Our findings indicate that the primary modes of interaction between NLRP3 and AGP involve salt bridge formation, hydrogen bonding, and hydrophobic interactions. Notably, no prior studies have explored the ligand–target interactions between AGP and the NLRP3 inflammasome pathway, as far as our knowledge extends.

There are several limitations in this study that warrant attention. Future investigations should include the use of a positive control drug for NLRP3 inhibition and the utilization of a mice model with NLRP3 gene knockout to validate the findings. Additionally, while the molecular docking results demonstrated favorable binding affinity between AGP and the targets of the NLRP3 pathway (all ≤ -5 kcal/mol), further exploration of efficacy and mechanism through site-directed mutagenesis is necessary to provide a more comprehensive understanding. Thirdly, our study laid the foundation for clinical efficacy studies of AGP in patients with AECOPD, which needs further investigation for its application on clinical practice.

Conclusion

In conclusion, the NLRP3 inflammasome activation has been implicated in the pathogenesis of AECOPD. Experimental evidence from in vivo and in vitro studies supports the potential of AGP to mitigate NLRP3 inflammasome activation and attenuate the inflammatory response during AECOPD. Currently, there is a lack of specific anti-inflammatory therapies targeting NLRP3 inflammasome in COPD, and the use of non-specific corticosteroids is associated with various side effects. AGP emerges as a promisingly natural compound as regulators of NLRP3 inflammasome that

might be used as an anti-inflammatory therapeutic strategy for AECOPD deserving further clinical investigations to determine its efficacy.

Abbreviations

AECOPD, acute exacerbation of chronic obstructive pulmonary disease; AGP andrographolide; ASC/PYCARD, apoptosis-associated speck-like containing a CARD; BALF, bronchoalveolar lavage fluid; Caspase-1, cysteinyl aspartate-specific protease-1; Cchord, chord compliance; COPD, chronic obstructive pulmonary disease; DMSO, dimethyl sulfoxide; ELISA, enzyme-linked immunosorbent assay; FEV100, forced expiratory volume at 100 ms; FEV200, forced expiratory volume at 200 ms; FRC, functional residual capacity; FVC, forced vital capacity; LPS, lipopolysaccharide; MLI, mean linear intercept; NLRP3, nucleotide-binding oligomerization domain-like receptor protein 3; IL, interleukin; PBS, phosphate buffer saline; PMA, phorbol 12-myristate 13-acetate; RT-qPCR, reverse transcription quantitative polymerase chain reaction; siRNA, small interfering RNA; TLC, total lung capacity; TCM, traditional Chinese medicine.

Acknowledgments

Thanks to Dr. Jun Chen from the Division of Pulmonary Diseases, State Key Laboratory of Biotherapy, West China Hospital, Sichuan University for his assistance to our experiment.

Funding

This work was financially supported by grants from the National Natural Science Foundation of China (No. 81400030, No. 82174139), and 1.3.5 project for disciplines of excellence, West China Hospital, Sichuan University (No. 2018-119).

Disclosure

The authors declare that they have no competing interests.

References

1. Singh D, Agusti A, Anzueto A, et al. Global strategy for the diagnosis, management, and prevention of chronic obstructive lung disease: the GOLD science committee report 2019. *Eur Respir J*. 2019;53(5):1900164. doi:10.1183/13993003.00164-2019
2. Venkatesan P. GOLD COPD report: 2023 update. *Lancet Respir Med*. 2023;11(1):18. doi:10.1016/s2213-2600(22)00494-5
3. Wang C, Xu J, Yang L, et al. Prevalence and risk factors of chronic obstructive pulmonary disease in China (the China Pulmonary Health [CPH] study): a national cross-sectional study. *Lancet*. 2018;391(10131):1706–1717. doi:10.1016/s0140-6736(18)30841-9
4. World Health Organization. The top 10 causes of death. Available from: https://www.who.int/news-room/fact-sheets/detail/the-top-10-causes-of-death. Accessed June 5, 2023.
5. Wedzicha JA, Seemungal TA. COPD exacerbations: defining their cause and prevention. *Lancet*. 2007;370(9589):786–796. doi:10.1016/s0140-6736(07)61382-8
6. Donaldson GC, Seemungal TA, Bhowmik A, Wedzicha JA. Relationship between exacerbation frequency and lung function decline in chronic obstructive pulmonary disease. *Thorax*. 2002;57(10):847–852. doi:10.1136/thorax.57.10.847
7. Seemungal TA, Donaldson GC, Paul EA, Bestall JC, Jeffries DJ, Wedzicha JA. Effect of exacerbation on quality of life in patients with chronic obstructive pulmonary disease. *Am J Respir Crit Care Med*. 1998;157(5 Pt 1):1418–1422. doi:10.1164/ajrccm.157.5.9709032
8. Soler-Cataluña JJ, Martínez-García MA, Román Sánchez P, Salcedo E, Navarro M, Ochando R. Severe acute exacerbations and mortality in patients with chronic obstructive pulmonary disease. *Thorax*. 2005;60(11):925–931. doi:10.1136/thx.2005.040527
9. Ko FW, Chan KP, Hui DS, et al. Acute exacerbation of COPD. *Respirology*. 2016;21(7):1152–1165. doi:10.1111/resp.12780
10. Walters JA, Tan DJ, White CJ, Gibson PG, Wood-Baker R, Walters EH. Systemic corticosteroids for acute exacerbations of chronic obstructive pulmonary disease. *Cochrane Database Syst Rev*. 2014;9:Cd001288. doi:10.1002/14651858.CD001288.pub4
11. Sayiner A, Aytemur ZA, Cirit M, Unsal İ. Systemic glucocorticoids in severe exacerbations of COPD. *Chest*. 2001;119(3):726–730. doi:10.1378/chest.119.3.726
12. Sharma BR, Kanneganti TD. NLRP3 inflammasome in cancer and metabolic diseases. *Nat Immunol*. 2021;22(5):550–559. doi:10.1038/s41590-021-00886-5
13. Malik A, Kanneganti TD. Inflammasome activation and assembly at a glance. *J Cell Sci*. 2017;130(23):3955–3963. doi:10.1242/jcs.207365
14. Proell M, Gerlic M, Mace PD, Reed JC, Riedl SJ. The CARD plays a critical role in ASC foci formation and inflammasome signalling. *Biochem J*. 2013;449(3):613–621. doi:10.1042/bj20121198
15. Colarusso C, Terlizzi M, Molino A, Pinto A, Sorrentino R. Role of the inflammasome in chronic obstructive pulmonary disease (COPD). *Oncotarget*. 2017;8(47):81813–81824. doi:10.18632/oncotarget.17850
16. Latz E, Xiao TS, Stutz A. Activation and regulation of the inflammasomes. *Nat Rev Immunol*. 2013;13(6):397–411. doi:10.1038/nri3452
17. Arend WP, Palmer G, Gabay C. IL-1, IL-18, and IL-33 families of cytokines. *Immunol Rev*. 2008;223:20–38. doi:10.1111/j.1600-065X.2008.00624.x

18. Wang H, Lv C, Wang S, Ying H, Weng Y, Yu W. NLRP3 Inflammasome Involves in the Acute Exacerbation of Patients with Chronic Obstructive Pulmonary Disease. *Inflammation*. 2018;41(4):1321–1333. doi:10.1007/s10753-018-0780-0
19. Li M, Hua Q, Shao Y, et al. Circular RNA circBbs9 promotes PM(2.5)-induced lung inflammation in mice via NLRP3 inflammasome activation. *Environ Int*. 2020;143:105976. doi:10.1016/j.envint.2020.105976
20. Nachmias N, Langier S, Brzezinski RY, et al. NLRP3 inflammasome activity is upregulated in an in-vitro model of COPD exacerbation. *PLoS One*. 2019;14(5):e0214622. doi:10.1371/journal.pone.0214622
21. Faner R, Sobradillo P, Noguera A, et al. The inflammasome pathway in stable COPD and acute exacerbations. *ERJ Open Res*. 2016;2(3). doi:10.1183/23120541.00002-2016
22. Ji S, Dai MY, Huang Y, et al. Influenza a virus triggers acute exacerbation of chronic obstructive pulmonary disease by increasing proinflammatory cytokines secretion via NLRP3 inflammasome activation. *J Inflamm*. 2022;19(1):8. doi:10.1186/s12950-022-00305-y
23. Zhang J, Xu Q, Sun W, Zhou X, Fu D, Mao L. New insights into the role of NLRP3 inflammasome in pathogenesis and treatment of chronic obstructive pulmonary disease. *J Inflamm Res*. 2021;14:4155–4168. doi:10.2147/jir.S324323
24. Akbar S. Andrographis paniculata: a review of pharmacological activities and clinical effects. *Altern Med Rev*. 2011;16(1):66–77.
25. Lim JC, Chan TK, Ng DS, Sagineedu SR, Stanslas J, Wong WS. Andrographolide and its analogues: versatile bioactive molecules for combating inflammation and cancer. *Clin Exp Pharmacol Physiol*. 2012;39(3):300–310. doi:10.1111/j.1440-1681.2011.05633.x
26. Tan WSD, Liao W, Zhou S, Wong WSF. Is there a future for andrographolide to be an anti-inflammatory drug? Deciphering its major mechanisms of action. *Biochem Pharmacol*. 2017;139:71–81. doi:10.1016/j.bcp.2017.03.024
27. Ding Y, Chen L, Wu W, Yang J, Yang Z, Liu S. Andrographolide inhibits influenza A virus-induced inflammation in a murine model through NF-κB and JAK-STAT signaling pathway. *Microbes Infect*. 2017;19(12):605–615. doi:10.1016/j.micinf.2017.08.009
28. Li J, Luo L, Wang X, Liao B, Li G. Inhibition of NF-kappaB expression and allergen-induced airway inflammation in a mouse allergic asthma model by andrographolide. *Cell Mol Immunol*. 2009;6(5):381–385. doi:10.1038/cmi.2009.49
29. Duan MX, Zhou H, Wu QQ, et al. Andrographolide protects against HG-induced inflammation, apoptosis, migration, and impairment of angiogenesis via PI3K/AKT-eNOS signalling in HUVECs. *Mediators Inflamm*. 2019;2019:6168340. doi:10.1155/2019/6168340
30. Wong SY, Tan MG, Wong PT, Herr DR, Lai MK. Andrographolide induces Nrf2 and heme oxygenase 1 in astrocytes by activating p38 MAPK and ERK. *J Neuroinflammation*. 2016;13(1):251. doi:10.1186/s12974-016-0723-3
31. Yen CC, Lii CK, Chen CC, et al. Andrographolide inhibits lipotoxicity-induced activation of the NLRP3 inflammasome in bone marrow-derived macrophages. *Am J Chin Med*. 2023;51(1):129–147. doi:10.1142/s0192415x23500088
32. He W, Sun J, Zhang Q, et al. Andrographolide exerts anti-inflammatory effects in Mycobacterium tuberculosis-infected macrophages by regulating the Notch1/Akt/NF-κB axis. *J Leukoc Biol*. 2020;108(6):1747–1764. doi:10.1002/jlb.3ma1119-584rrr
33. Zhang XF, Ding MJ, Cheng C, et al. Andrographolide attenuates oxidative stress injury in cigarette smoke extract exposed macrophages through inhibiting SIRT1/ERK signaling. *Int Immunopharmacol*. 2020;81:106230. doi:10.1016/j.intimp.2020.106230
34. Tan WS, Peh HY, Liao W, et al. Cigarette smoke-induced lung disease predisposes to more severe infection with nontypeable Haemophilus influenzae: protective effects of andrographolide. *J Nat Prod*. 2016;79(5):1308–1315. doi:10.1021/acs.jnatprod.5b01006
35. Barrett EG, Wilder JA, March TH, Espindola T, Bice DE. Cigarette smoke-induced airway hyperresponsiveness is not dependent on elevated immunoglobulin and eosinophilic inflammation in a mouse model of allergic airway disease. *Am J Respir Crit Care Med*. 2002;165(10):1410–1418. doi:10.1164/rccm.2106029
36. Kim RY, Pinkerton JW, Gibson PG, Cooper MA, Horvat JC, Hansbro PM. Inflammasomes in COPD and neutrophilic asthma. *Thorax*. 2015;70 (12):1199–1201. doi:10.1136/thoraxjnl-2014-206736
37. Leszczyńska K, Jakubczyk D, Górska S. The NLRP3 inflammasome as a new target in respiratory disorders treatment. *Front Immunol*. 2022;13:1006654. doi:10.3389/fimmu.2022.1006654
38. Ma Y, Long Y, Chen Y. Roles of inflammasome in cigarette smoke-related diseases and physiopathological disorders: mechanisms and therapeutic opportunities. *Front Immunol*. 2021;12:720049. doi:10.3389/fimmu.2021.720049
39. Ji S, Bai Q, Wu X, et al. Unique synergistic antiviral effects of Shufeng Jiedu Capsule and oseltamivir in influenza A viral-induced acute exacerbation of chronic obstructive pulmonary disease. *Biomed Pharmacother*. 2020;121:109652. doi:10.1016/j.biopha.2019.109652
40. Bafadhel M, McKenna S, Terry S, et al. Acute exacerbations of chronic obstructive pulmonary disease: identification of biologic clusters and their biomarkers. *Am J Respir Crit Care Med*. 2011;184(6):662–671. doi:10.1164/rccm.201104-0597OC
41. Fu JJ, McDonald VM, Baines KJ, Gibson PG. Airway IL-1β and systemic inflammation as predictors of future exacerbation risk in asthma and COPD. *Chest*. 2015;148(3):618–629. doi:10.1378/chest.14-2337
42. Zou Y, Chen X, Liu J, et al. Serum IL-1β and IL-17 levels in patients with COPD: associations with clinical parameters. *Int J Chron Obstruct Pulmon Dis*. 2017;12:1247–1254. doi:10.2147/copd.S131877
43. Churg A, Zhou S, Wang X, Wang R, Wright JL. The role of interleukin-1beta in murine cigarette smoke-induced emphysema and small airway remodeling. *Am J Respir Cell Mol Biol*. 2009;40(4):482–490. doi:10.1165/rcmb.2008-0038OC
44. Doz E, Noulin N, Boichot E, et al. Cigarette smoke-induced pulmonary inflammation is TLR4/MyD88 and IL-1R1/MyD88 signaling dependent. *J Immunol*. 2008;180(2):1169–1178. doi:10.4049/jimmunol.180.2.1169
45. Zhong Y, Kinio A, Saleh M. Functions of NOD-like receptors in human diseases. *Front Immunol*. 2013;4:333. doi:10.3389/fimmu.2013.00333
46. Akata K, van Eeden SF. Lung macrophage functional properties in chronic obstructive pulmonary disease. *Int J Mol Sci*. 2020;21(3). doi:10.3390/ijms21030853
47. Lee JW, Chun W, Lee HJ, et al. The role of macrophages in the development of acute and chronic inflammatory lung diseases. *Cells*. 2021;10(4). doi:10.3390/cells10040897
48. Chen X, Tang J, Shuai W, Meng J, Feng J, Han Z. Macrophage polarization and its role in the pathogenesis of acute lung injury/acute respiratory distress syndrome. *Inflamm Res*. 2020;69(9):883–895. doi:10.1007/s00011-020-01378-2
49. Aggarwal NR, King LS, D'Alessio FR. Diverse macrophage populations mediate acute lung inflammation and resolution. *Am J Physiol Lung Cell Mol Physiol*. 2014;306(8):L709–25. doi:10.1152/ajplung.00341.2013
50. Hayman YA, Sadofsky LR, Williamson JD, Hart SP, Morice AH. The effects of exogenous lipid on THP-1 cells: an in vitro model of airway aspiration? *ERJ Open Res*. 2017;3(1). doi:10.1183/23120541.00026-2016

51. Heulens N, Korf H, Mathyssen C, et al. 1,25-Dihydroxyvitamin D modulates antibacterial and inflammatory response in human cigarette smoke-exposed macrophages. *PLoS One*. 2016;11(8):e0160482. doi:10.1371/journal.pone.0160482
52. Liu C, Wang M, Sun W, et al. PU.1 serves a critical role in the innate defense against Aspergillus fumigatus via dendritic cell-associated C-type lectin receptor-1 and toll-like receptors-2 and 4 in THP-1-derived macrophages. *Mol Med Rep*. 2017;15(6):4084–4092. doi:10.3892/mmr.2017.6504
53. Kumar H, Kumagai Y, Tsuchida T, et al. Involvement of the NLRP3 inflammasome in innate and humoral adaptive immune responses to fungal beta-glucan. *J Immunol*. 2009;183(12):8061–8067. doi:10.4049/jimmunol.0902477
54. McNeela EA, Burke A, Neill DR, et al. Pneumolysin activates the NLRP3 inflammasome and promotes proinflammatory cytokines independently of TLR4. *PLoS Pathog*. 2010;6(11):e1001191. doi:10.1371/journal.ppat.1001191
55. Rotta Detto Loria J, Rohmann K, Droemann D, et al. Nontypeable Haemophilus influenzae infection upregulates the NLRP3 inflammasome and leads to Caspase-1-dependent secretion of Interleukin-1β - a possible pathway of exacerbations in COPD. *PLoS One*. 2013;8(6):e66818. doi:10.1371/journal.pone.0066818
56. Tate MD, Ong JDH, Dowling JK, et al. Reassessing the role of the NLRP3 inflammasome during pathogenic influenza A virus infection via temporal inhibition. *Sci Rep*. 2016;6:27912. doi:10.1038/srep27912
57. Płóciennikowska A, Hromada-Judycka A, Borzęcka K, Kwiatkowska K. Co-operation of TLR4 and raft proteins in LPS-induced pro-inflammatory signaling. *Cell Mol Life Sci*. 2015;72(3):557–581. doi:10.1007/s00018-014-1762-5
58. Kelley N, Jeltema D, Duan Y, He Y. The NLRP3 inflammasome: an overview of mechanisms of activation and regulation. *Int J Mol Sci*. 2019;20(13). doi:10.3390/ijms20133328
59. Cao Y, Zhou X, Yin Z, et al. The anti-inflammatory effect of BML-111 on COPD may be mediated by regulating NLRP3 inflammasome activation and ROS production. *Prostaglandins Other Lipid Mediat*. 2018;138:23–30. doi:10.1016/j.prostaglandins.2018.08.001
60. Mahalanobish S, Dutta S, Saha S, Sil PC. Melatonin induced suppression of ER stress and mitochondrial dysfunction inhibited NLRP3 inflammasome activation in COPD mice. *Food Chem Toxicol*. 2020;144:111588. doi:10.1016/j.fct.2020.111588
61. Peng Z, Zhang W, Qiao J, He B. Melatonin attenuates airway inflammation via SIRT1 dependent inhibition of NLRP3 inflammasome and IL-1β in rats with COPD. *Int Immunopharmacol*. 2018;62:23–28. doi:10.1016/j.intimp.2018.06.033
62. Tian Q, Xu M, He B. Histidine ameliorates elastase- and lipopolysaccharide-induced lung inflammation by inhibiting the activation of the NLRP3 inflammasome. *Acta Biochim Biophys Sin*. 2021;53(8):1055–1064. doi:10.1093/abbs/gmab072
63. Tian X, Xue Y, Xie G, et al. (-)-Epicatechin ameliorates cigarette smoke-induced lung inflammation via inhibiting ROS/NLRP3 inflammasome pathway in rats with COPD. *Toxicol Appl Pharmacol*. 2021;429:115674. doi:10.1016/j.taap.2021.115674
64. Wang L, Chen Q, Yu Q, Xiao J, Zhao H. TREM-1 aggravates chronic obstructive pulmonary disease development via activation NLRP3 inflammasome-mediated pyroptosis. *Inflamm Res*. 2021;70(9):971–980. doi:10.1007/s00011-021-01490-x
65. Wang L, Lei W, Zhang S, Yao L. MCC950, a NLRP3 inhibitor, ameliorates lipopolysaccharide-induced lung inflammation in mice. *Bioorg Med Chem*. 2021;30:115954. doi:10.1016/j.bmc.2020.115954
66. Zhang MY, Jiang YX, Yang YC, et al. Cigarette smoke extract induces pyroptosis in human bronchial epithelial cells through the ROS/NLRP3/caspase-1 pathway. *Life Sci*. 2021;269:119090. doi:10.1016/j.lfs.2021.119090
67. Calverley PMA, Sethi S, Dawson M, et al. A randomised, placebo-controlled trial of anti-interleukin-1 receptor 1 monoclonal antibody MEDI8968 in chronic obstructive pulmonary disease. *Respir Res*. 2017;18(1):153. doi:10.1186/s12931-017-0633-7
68. MedImmune. A study to evaluate the safety of MEDI2338 in subjects with chronic obstructive pulmonary disease. Available from: https://clinicaltrials.gov/ct2/show/NCT01322594. Accessed May 16, 2024.
69. Novartis. Safety And efficacy of multiple doses of canakinumab (ACZ885) in chronic obstructive pulmonary disease (COPD) patients. Available from: https://clinicaltrials.gov/ct2/show/NCT00581945. Accessed May 16, 2024.
70. Coll RC, Robertson AA, Chae JJ, et al. A small-molecule inhibitor of the NLRP3 inflammasome for the treatment of inflammatory diseases. *Nat Med*. 2015;21(3):248–255. doi:10.1038/nm.3806
71. Madurka I, Vishnevsky A, Soriano JB, et al. DFV890: a new oral NLRP3 inhibitor-tested in an early phase 2a randomised clinical trial in patients with COVID-19 pneumonia and impaired respiratory function. *Infection*. 2023;51(3):641–654. doi:10.1007/s15010-022-01904-w
72. Islam MT, Ali ES, Uddin SJ, et al. Andrographolide, a diterpene lactone from Andrographis paniculata and its therapeutic promises in cancer. *Cancer Lett*. 2018;420:129–145. doi:10.1016/j.canlet.2018.01.074
73. Li J, Xie Y, Zhao P, et al. A Chinese herbal formula ameliorates COPD by inhibiting the inflammatory response via downregulation of p65, JNK, and p38. *Phytomedicine*. 2021;83:153475. doi:10.1016/j.phymed.2021.153475
74. Tao L, Lu X, Fu Z, et al. Tong Sai granule improves AECOPD via regulation of MAPK-SIRT1-NF-κB pathway and cellular senescence alleviation. *J Ethnopharmacol*. 2023;314:116622. doi:10.1016/j.jep.2023.116622
75. Lu F, Yang H, Lin SD, et al. Cyclic peptide extracts derived from Pseudostellaria heterophylla ameliorates COPD via regulation of the TLR4/MyD88 pathway proteins. *Front Pharmacol*. 2020;11:850. doi:10.3389/fphar.2020.00850
76. Pinzi L, Rastelli G. Molecular docking: shifting paradigms in drug discovery. *Int J Mol Sci*. 2019;20(18):4331. doi:10.3390/ijms20184331